



**HAL**  
open science

## Thoracic Outlet Syndrome: Diagnostic Accuracy of MRI

Alexandre Hardy, Cécile Pougès, Guillaume Wavreille, Hélène Behal, Xavier Demondion, Guillaume Lefebvre

### ► To cite this version:

Alexandre Hardy, Cécile Pougès, Guillaume Wavreille, Hélène Behal, Xavier Demondion, et al.. Thoracic Outlet Syndrome: Diagnostic Accuracy of MRI. *Orthopaedics & Traumatology: Surgery & Research*, 2019, 105, pp.1563 - 1569. 10.1016/j.otsr.2019.09.020 . hal-03489181

**HAL Id: hal-03489181**

**<https://hal.science/hal-03489181>**

Submitted on 21 Jul 2022

**HAL** is a multi-disciplinary open access archive for the deposit and dissemination of scientific research documents, whether they are published or not. The documents may come from teaching and research institutions in France or abroad, or from public or private research centers.

L'archive ouverte pluridisciplinaire **HAL**, est destinée au dépôt et à la diffusion de documents scientifiques de niveau recherche, publiés ou non, émanant des établissements d'enseignement et de recherche français ou étrangers, des laboratoires publics ou privés.



Distributed under a Creative Commons Attribution - NonCommercial 4.0 International License

## Thoracic Outlet Syndrome: Diagnostic Accuracy of MRI

Alexandre **Hardy**<sup>a,b,\*</sup>, Cécile **Pougès**<sup>c</sup>, Guillaume **Wavreille**<sup>d</sup>, Hélène **Behal**<sup>b,e</sup>, Xavier **Demondion**<sup>b,f,g</sup>, Guillaume **Lefebvre**<sup>b,f</sup>

a Service de Chirurgie Orthopédique et Traumatologique, Hôpital Salengro, CHRU de Lille, Rue Emile Laisne, 59000, Lille, France

b Université Lille-Hauts de France, 59000 Lille, France

c Service de chirurgie Orthopédique et Traumatologique, Hôpital Saint Vincent de Paul, Boulevard de Belfort, 59000 Lille, France

d Clinique Lille Sud 96 rue Gustave Delory 59810 Lesquin, France

e Santé publique : épidémiologie et qualité des soins, Unité de Biostatistiques, CHRU de Lille, Rue Emile Laisne, 59000, Lille, France

f Service d'Imagerie musculo-squelettique, Hôpital Salengro, CHRU de Lille, Rue Emile Laisne, 59000, Lille, France

g Laboratoire d'Anatomie et d'Organogénèse, Faculté de Médecine, Place de Verdun, 59000 Lille, France

**\*Corresponding author:** Alexandre Thomas Hardy, Service de Chirurgie Orthopédique et Traumatologique, Hôpital Salengro, CHRU de Lille, Rue Emile Laisne, 59037, Lille, FRANCE

Tel.: +33 320 446 828

Fax: +33 320 446 607

E-mail: al.hardy@hotmail.fr

## **ABSTRACT**

**Background:** Thoracic outlet syndrome (TOS) is challenging to diagnose, as the physical findings and investigations lack sensitivity and/or specificity. Magnetic resonance imaging (MRI) with dynamic manoeuvres can rule out a tumour and detect anatomical abnormalities potentially responsible for compression. The objective of this study was to assess the sensitivity and specificity of MRI for identifying anatomical structures responsible for compression in TOS, using intra-operative findings as the diagnostic reference standard.

**Hypothesis:** MRI is effective in diagnosing the source of compression in TOS, notably within the scalene triangle and at the pleural apex.

**Methods:** We retrospectively included 48 patients who underwent surgery for TOS after a work-up that included MRI (1.5-T, n=29 and 3-T, n=19). The MRI scans were reviewed for the study by a specialised radiologist who was unaware of the intra-operative findings. The sensitivity and specificity of MRI for diagnosing TOS were estimated using the intra-operative findings as the reference standard.

**Results:** MRI identified a structure potentially responsible for TOS in 34 (71%) patients; thus, the false-negative rate was 14/48 (29%). The sensitivity of MRI was 28% for compression at the suspensory ligament of the pleural dome, 81% for hypertrophy of the anterior scalene muscle, and 50% for an accessory scalene muscle. For diagnosing a cervical rib, MRI had 100% sensitivity and 100% specificity.

**Conclusion:** MRI can contribute to the diagnosis of TOS. Specificity is sufficiently high to provide guidance for planning the surgical procedure. Sensitivity, however, is too low for MRI to be useful as a screening test. MRI should be used in combination with the clinical assessment and other investigations to assist in the diagnosis of TOS.

**Level of evidence:** IV, retrospective cohort study

**Key words:** Thoracic outlet syndrome. Magnetic resonance imaging. Diagnosis.

## 1 Introduction

Thoracic outlet syndrome is characterised by vascular and/or neurological symptoms caused by compression of the subclavian vessels and brachial plexus as they exit the chest cavity towards the arm. Compression can occur at various sites in the thoracic outlet, including the superior pleural sinus (due to ligaments issuing from C7 and the first rib, which can attach to the suprapleural membrane), the scalene triangle between the anterior and middle scalene muscles, the costoclavicular space (between the first rib and clavicle), and the retro-pectoralis minor space (between the subscapularis and pectoralis minor muscle) [1-2]. TOS may manifest as neurological and/or vascular symptoms. Uncomplicated TOS, defined as TOS without neurological deficits or vascular thrombosis, is diagnosed based on a set of converging data from the physical examination and investigations, combined with the absence of evidence of an alternative diagnosis. None of the available investigations have 100% sensitivity and specificity. The work-up consists of radiographs of the cervical spine, dynamic Doppler ultrasonography or computed tomography (CT)-angiography, an electrodiagnostic study, and magnetic resonance imaging (MRI), notably when the neurological manifestations predominate.

Dynamic Doppler ultrasonography has been proven effective in diagnosing vascular compression in the costoclavicular space by showing a stenosis, a post-stenotic aneurysm, or a zone of partial thrombosis [3]. However, no investigation has been found effective in identifying structures responsible for compression at the pleural apex or scalene triangle.

MRI with acquisitions during postural manoeuvres can detect compression of neurological and vascular structures and identify the anatomical abnormalities causing the compression [4]. Recent advances in MRI technology, including the advent of 3-T MRI, have improved spatial resolution and diminished acquisition times by increasing the signal-to-noise

ratio. Thus, 3-T MRI has a marked advantage over 1.5-T MRI for investigating axial and peripheral musculoskeletal abnormalities [5]. Nonetheless, few data are available on the diagnostic performance of MRI in patients with TOS. We are aware of a single published study, in which 1.5-T MRI failed to contribute meaningfully to the diagnosis of TOS [6].

TOS is often treated non-operatively, using physical therapy. When the symptoms persist, however, surgery may be offered. If MRI were found to be effective in detecting structures responsible for compression in the scalene triangle and at the superior pleural sinus, it would constitute an aid not only for diagnosing TOS but also for the planning the surgical procedure.

The primary objective of this study was to assess the sensitivity and specificity of MRI for detecting anatomical structures responsible for compression in TOS, using intra-operative findings as the diagnostic reference standard. The secondary objective was to compare the diagnostic performance of 1.5-T vs. 3-T MRI for identifying the structures responsible for compression. The working hypothesis was that MRI is effective in diagnosing the source of compression in TOS, notably within the scalene triangle and at the superior pleural sinus.

## **2 Material and Methods**

### **2.1 Patients**

The inclusion criteria were a history of surgery for TOS after a work-up that included MRI of the thoracic outlet. Written informed consent was obtained from each patient before study inclusion. Patients were routinely asked about contra-indications to MRI. The following data were collected for each patient: body weight, height, age, medical history, and reason for the investigation.

All the study patients underwent TOS surgery between 2012 and 2016 by the same orthopaedic surgeon specialised in the upper limb and peripheral nerves. In all patients, the pre-operative work-up included an MRI scan, an electrodiagnostic study, antero-posterior and lateral radiographs of the cervical spine, and either a dynamic Doppler ultrasound scan or a CT-angiogram. Patients who had had surgery for TOS without first being investigated by MRI were excluded.

## **2.2 Surgical procedure**

The procedure was performed under general anaesthesia with the patient supine in the 30° semi-recumbent supine position and the head turned away from the affected side. The affected upper limb was left free in the operative field. A transverse supra-clavicular cervicotomy was performed routinely for the scalenectomy and release of the superior pleural sinus. When first rib resection was required, an infra-clavicular approach was performed also (Figure 1). All the structures responsible for compression were described in detail in the surgical report and on a data collection form.

## **2.3 MRI (Figures 2, 3, 4)**

Either 1.5-T or 3-T MRI was performed to assess the clinical suspicion of TOS. Images were acquired with the arm along the body then in 130° of abduction and external rotation. The head was in the neutral position. The images were acquired from the cervical spine to the humeral head.

All MRI scans were reviewed for the study by the same radiologist specialised in musculoskeletal imaging. The radiologist was unaware of the intra-operative findings and completed a standardised data collection form.

Parameters for the 1.5-T MRI scans (Siemens, Germany) were as follows: 30 T1- or T2-weighted sagittal slices 4 mm in thickness and MRI-angiography. For 3-T MRI (Ingenia, Philips Healthcare, The Netherlands), the parameters were as follows: 30 T1/T2 sagittal slices 3.5 mm in thickness; 3D TSE T1 - 0.6 mm isotropic sequences (350 slices); 3D TSE T2 STIR - 0.6 mm isotropic sequences (194 slices); post-gadolinium 3D gradient-echo – 1 mm isotropic sequences (100 slices); and MRI-angiography.

The standardised injection protocol consisted in an intravenous injection of gadolinium chelate (Dotarem<sup>®</sup> 0.5 mmol/mL, gadoteric acid, Laboratoire Guerbet, Villepinte, France), 0.2 mL/kg (0.1 mmol/kg), in the symptom-free upper limb or, when the symptoms were bilateral, in the upper limb where the symptoms were mildest.

## **2.4 Data collection**

An array of findings were looked for in the MRI and surgical reports. The site of the compression was recorded as the scalene triangle (bordered by the posterior edge of the anterior scalene muscle, anterior edge of the middle scalene muscle, and upper aspect of the first rib), the costoclavicular space (between the first rib and the clavicle), or the pectoralis minor space (behind the pectoralis minor muscle). Compression could occur at more than one site. In some cases, the site of compression was not identified.

The following criteria were used to assess the presence or absence of extrinsic compression by bony or fibromuscular structures:

- A fibrous band belonging to the pleural dome suspensory system: transverse septo-costal ligament, costo-septo-costal ligament, or vertebro-septo-costal ligament, seen by MRI as linear low signal on the T1-weighted sequence in an orientation that differed from that of the muscle fibres;
- Cervical rib under C7 and above C8;



- Hypertrophic C7 transverse process, defined as a C7 transverse process larger than the T1 transverse process by MRI;
- Abnormal shape or malunion of the clavicle or first rib by MRI (Figure 5);
- Hypertrophy of the anterior scalene muscle defined as an antero-posterior diameter greater than 10 mm and/or as the absence of a band of fat by MRI; the surgical definition was sufficient anterior scalene muscle bulk to completely mask the subclavian artery (Figure 6);
- A fibrous band from the anterior scalene muscle seen by MRI as low T1 signal within the muscle;
- Hypertrophy of the middle scalene muscle defined as an antero-posterior diameter greater than 10 mm and/or as the absence of a band of fat by MRI; the surgical definition was tenting of the C7 and/or C8 root or sufficient muscle bulk to mask the C8/T1 root;
- A fibrous band from the middle scalene muscle seen by MRI as low T1 signal within the muscle;
- An accessory scalene muscle or third scalene muscle in the scalene triangle, having fibres whose orientation differed from those of the anterior and middle scalene muscles by MRI; the abnormal muscle fibres could cross through the lower roots of the brachial plexus (Figure 7);
- Hypertrophy of the subclavius muscle defined as an antero-posterior diameter greater than 10 mm and/or a mass effect at the level of the subclavian vein by MRI; the surgical definition was persistent neuro-vascular compression with the arm abducted despite first rib resection;
- Hypertrophy of the pectoralis minor muscle was defined as an antero-posterior diameter greater than that of the pectoralis major by MRI; the surgical definition was persistent neuro-vascular compression after first rib resection;

- A mass effect of the coracoclavicular ligament in direct contact with the subclavian vein, which can cause direct compression in the clavicular-pectoral region.

The cut-offs used to define muscle hypertrophy were chosen based on mean muscle thickness values measured by Demondion et al. in healthy volunteers [4], i.e., 8.73 mm for the anterior scalene muscle in extreme abduction and 5 mm for the subclavius muscle. For our study, hypertrophy of the anterior and middle scalene muscles and subclavius muscle was defined as a thickness greater than 10 mm.

In general, nerve compression was defined as follows:

- By MRI, tenting or altered trajectory of the nerve promoted by the extrinsic compression, disappearance of the fat surrounding the nerve, and/or muscle hypertrophy as defined above;
- By surgery, altered gross appearance or decreased diameter of the nerve in contact with the structure causing compression, tenting or altered trajectory of the nerve promoted by the extrinsic compression, accessory structure seen along the course of the nerve, and/or muscle hypertrophy as defined above.

## **2.5 Statistical analysis**

The sensitivity, specificity, positive predictive value (PPV), and negative predictive value (NPV) of the MRI findings for the diagnosis of TOS were computed using the intra-operative findings as the reference standard. The 95% confidence interval (95%CI) was estimated for sensitivity and specificity values that were not equal to 0% or 100%. Excel (Microsoft, Redmond, WA, USA) was used for the statistical analysis.

## **3 Results**

### **3.1 Diagnostic performance of MRI (Tables 1 and 2)**

The study included 48 cases of TOS in 46 patients, 36 (78.3%) females and 10 (21.7%) males ranging in age from 22 to 67 years (mean age, 40.1±10.6 years). The TOS was unilateral in 44 patients and bilateral in 2 patients. The right side was involved in 27 cases and the left side in 21 cases.

The pre-operative MRI scan was performed using a 1.5-T machine in 29 patients and a 3-T machine in 19 patients.

During surgery, extrinsic compression by bony or muscular structures was found in all cases, justifying the treatment decision. By MRI, extrinsic compression by bony or muscular structures was visualized in 34 (71%) cases. The remaining 14 (29%) MRI scans that were considered normal were false-negative tests. In these patients, the decision to perform surgery was based on abnormal findings from dynamic Doppler ultrasonography and/or CT-angiography.

During surgery, compression was found at more than one site in 44 (92%) case and in the scalene triangle only in 4 (8%) cases. No patient had compression located only in the costoclavicular space or retro-pectoralis minor space (Table 1). MRI showed compression at more than one site in 10 (21%) cases, compression in the scalene triangle only in 21 (44%) cases, and compression in the costoclavicular space in 3 (6%) cases. No patient had MRI evidence of compression confined to the retro-pectoralis minor space. In 14 (29%) cases, the structure responsible for compression was not identified and the site of compression was therefore recorded by the radiologist as not determined.

### **Superior pleural sinus**

Compression by fibrous bands was identified in 63 cases during surgery and in 10 cases by MRI. Thus, for detecting this cause of compression MRI had 28% (95%CI, 13%-42%) sensitivity and 100% specificity.

### **Scalene triangle and costoclavicular space**

Anterior scalene muscle hypertrophy was found in 26 cases by surgery and 25 cases by MRI, yielding 81% (95%CI, 65%-95%) sensitivity and 82% (95%CI, 65%-97%) specificity. Middle scalene muscle hypertrophy was apparent during surgery in 33 cases and by MRI in only 13 cases, yielding 39% (95%CI, 22%-56%) sensitivity and 100% specificity. Fibrous components of the anterior scalene muscle were seen in 26 cases during surgery and in a single case by MRI (specificity, 95% [86%-100%]); the corresponding data for the middle scalene muscle were 11 cases by surgery and none by MRI (100% specificity). An accessory or third scalene muscle was identified in the scalene triangle in 8 cases by surgery and 4 cases by MRI, yielding 50% sensitivity (95%CI, 15%-84%) and 100% specificity. Finally, hypertrophy of the subclavius muscle was noted in 3 cases by surgery and in 7 cases by MRI, yielding 100% sensitivity and 91% (95%CI, 82%-99%) specificity.

### **Retro-pectoralis minor space**

Compression due to hypertrophy of the pectoralis minor muscle was found during surgery in 1 case and by MRI in 4 cases, yielding 100% sensitivity and 94% (95%CI, 86%-100%) specificity. Hypertrophy of the subclavius and pectoralis minor muscles was either over-diagnosed by MRI or seen during surgery but deemed not to cause compression and therefore left unrecorded in the surgical report. The PPV (likelihood that one of these factors was recorded by the surgeon as causing compression if seen by MRI) was 43% for the subclavius muscle and 25% for the pectoralis minor muscle.

During surgery, the coracoclavicular ligament was found to cause compression of the subclavian vein. In no case was the coracoclavicular ligament considered to cause compression by MRI (100% specificity).

### **Compression by bony structures**

In 3 cases, MRI showed cervical ribs, for which surgical resection was required (100% sensitivity and 100% specificity). No cases of clavicular malunion or transverse process hypertrophy were found during surgery or by MRI.

Neither sensitivity nor the PPV were computed for the findings that were not correctly identified by MRI (VP=0), i.e., transverse process hypertrophy, abnormality of a rib or clavicle, compression by the coracoclavicular ligament, and fibrous component of the anterior or middle scalene muscle.

### **3.2 Comparison of 1.5-T and 3-T MRI (Table 3)**

Sensitivity and specificity were estimated separately for 1.5-T MRI and 3-T MRI when comparable criteria were available. Of the 48 cases, 29 were investigated using 1.5-T MRI and 19 using 3-T MRI.

Sensitivity and specificity were higher with 3-T than with 1.5-T MRI for all the criteria studied except compression by fibrous bands, for which sensitivity was higher by 1.5-T MRI (33% vs. 16% by 3-T MRI). Sensitivity was higher by 3-T MRI than by 1.5-T MRI for diagnosing anterior scalene muscle hypertrophy (90% vs. 75%) and middle scalene muscle hypertrophy (50% vs. 33%). Specificity was also better with 3-T MRI for diagnosing anterior scalene muscle hypertrophy (89% vs. 77% with 1.5-T MRI), a fibrous component from the

anterior scalene muscle (100% vs. 95%), hypertrophy of the subclavius muscle (94% vs. 89%), and hypertrophy of the pectoralis minor muscle (100% vs. 90%).

The confidence intervals were not estimated, due to the small numbers of patients in each subgroup.

#### **4 DISCUSSION**

The multiplicity and variety of clinical presentations of TOS raise major diagnostic challenges. The diagnosis is most difficult in the absence of complications (vascular thrombosis or neurological deficit). The dynamic nature of the compression generates further difficulty. Thus the diagnosis of TOS is often controversial and must generally rely on a set of converging arguments from the clinical examination and investigations. Consequently, an assessment of the potential diagnostic usefulness of MRI was timely.

Our results show that MRI is a good test for confirming the diagnosis, with high specificities of 82% to 100% for the 12 sources of compression. In contrast, MRI did not perform well as a screening tool, as sensitivity was low for some sources of compression (28% for fibrous bands from the pleural dome suspensory system, 39% for hypertrophy of the middle scalene muscle, and 50% for an accessory scalene muscle). Overall sensitivity of MRI, however, was 71%. MRI had good sensitivity and specificity for some sources of compression including a cervical rib (100%), anterior scalene muscle hypertrophy (81%), subclavius muscle hypertrophy (100%), and pectoralis minor muscle hypertrophy (100%). However, MRI performed poorly for identifying fibrous components of the anterior and middle scalene muscles, determining that the coracoclavicular ligament caused compression, or identifying an abnormality of a rib or clavicle: none of these anomalies found during surgery was diagnosed on the pre-operative MRI scan.

The main limitation of our study is the retrospective design, which required that the surgical findings be obtained from the surgeon reports. Nevertheless, these reports provided extremely detailed descriptions of each structure that caused compression and was removed surgically. The sample size was too small for an extensive statistical comparison of 1.5-T vs. 3-T MRI. On the other hand, we were able to perform a satisfactory analysis of the performance of MRI for diagnosing each source of compression. In addition, to the best of our knowledge, this is the first study to compare the sensitivity and specificity of 1.5-T and 3-T MRI for the diagnosis of TOS and also reports the largest cohort, with 48 cases, comparing MRI and surgical findings in TOS[6]. The MRI scans were obtained according to a standard protocol but required good patient cooperation, as the postural manoeuvres were sometimes difficult to maintain, a factor that may have decreased the reproducibility of the test. Finally, that retropulsion was not feasible and the exploration was performed in the supine position may have minimised the postural component of the vascular compressions.

One source of imperfect correlations between MRI and surgical findings may be the difference in vision between the MRI slices and the dynamic perceptions during surgery. Furthermore, the criteria for compression that are applied during surgery have a subjective component and are therefore difficult to apply to MRI scans. The nature of some of the sources of compression resulted in poor MRI performance. Thus, structures measuring only about 1 mm, such as fibrous bands, were difficult to identify, movement artefacts related to the lung apex complicated the diagnosis of compression by the pleural dome suspensory system, and the low contrast of structures within the scalene triangle may explain the limited performance for compression by the middle scalene muscle.

MRI is only one of several investigations that can help to diagnose TOS. Advantages of MRI are lack of invasiveness, absence of exposure to ionising radiation, and good contrast

capable of differentiating various types of soft tissue. However, few published studies have assessed the diagnostic performance of MRI in TOS.

In a study by Demondion et al. [4], MRI findings in patients with symptomatic TOS included a narrower costoclavicular space, subclavius muscle hypertrophy, and a narrower retro-pectoralis minor space during postural manoeuvres compared to asymptomatic volunteers. Other studies have emphasised the dynamic nature of TOS and the importance of obtaining MRI acquisitions with the arm abducted, chiefly to ensure detection of vascular compression in the costoclavicular space[7-8]. Contrast medium injection was helpful for detecting vascular compression [9-11], and 3D reformation further enhanced the diagnosis[12]. Although MRI can detect vascular compression, dynamic Doppler ultrasonography remains the most informative investigation for confirming the existence of an arterial stenosis in the costoclavicular space. Thus, in the study reported by Demondion et al. [3], images obtained in the seated position with the arm abducted at 130° showed an arterial stenosis in 78% of symptomatic patients and 20% of asymptomatic volunteers.

Aralasmak et al. [2] found that MRI was effective in identifying muscle hypertrophy, an accessory muscle, or an abnormal muscle attachment at sites of compression in the thoracic outlet. Baumer et al. [13] reported that 3-T MRI contributed to the identification of compression at the pleural dome: bands responsible for compression were seen on the images then confirmed during surgery.

A single study, by Singh et al.[6], assessed the diagnostic performance of MRI using surgery as the reference standard. In this study, 1.5-T MRI was used, and sensitivity and specificity were computed only for overall MRI performance. The data from the 42 included cases showed that MRI and surgical findings agreed in only 17 (40%) cases. MRI had 41% sensitivity, 33% specificity, 89% PPV, and 4% NPV. Sensitivity and specificity were not estimated individually for each source of compression, in contrast to our study.



Our comparison of the performance of 1.5-T and 3-T MRI is only of descriptive value, as the sample sizes were too small to allow a statistical analysis. As expected, 3-T MRI seemed to perform better than 1.5-T MRI for diagnosing the sources of compression for which data were available from both techniques.

## **5 CONCLUSION**

MRI contributes to the diagnosis of TOS by identifying certain sources of compression, thereby assisting in pre-operative planning. MRI has satisfactory specificity, although its sensitivity is too low for use as a screening tool. MRI should be used in combination with the clinical findings and other investigations to optimise the diagnosis of TOS. Using a 3-T magnetic field may enhance diagnostic performance and deserves investigation in a larger number of patients.

### **Disclosure of interest**

None of the authors has any conflicts of interest to declare.

### **Funding**

None

### **Contributions of each author**

Alexandre Hardy: Author, final approbation of the study

Cécile Pougès designed and coordinated the study, drafted the manuscript, and revised the manuscript for important intellectual content.

Guillaume Wavreille performed the surgical procedures.

Hélène Béhal performed the statistical analysis.

Xavier Demondion designed the study.

Guillaume Lefebvre coordinated the study, reviewed the MRI scans, and drafted the manuscript.

## REFERENCES

- 1 Demondion X, Boutry N, Drizenko A, Paul C, Francke JP, Cotten A. Thoracic outlet: anatomic correlation with MR imaging. *American Journal of Roentgenology*. 2000 Aug;175(2):417–22.
- 2 Aralasmak A, Cevikol C, Karaali K, Senol U, Sharifov R, Kilicarslan R, et al. MRI findings in thoracic outlet syndrome. *Skeletal Radiol*. 2012 Jul 11;41(11):1365–74.
- 3 Demondion X, Vidal C, Herbinet P, Gautier C, Duquesnoy B, Cotten A. Ultrasonographic Assessment of Arterial Cross-sectional Area in the Thoracic Outlet on Postural Maneuvers Measured With Power Doppler Ultrasonography in Both Asymptomatic and Symptomatic Populations. *JUM*. 2006;25(2):217–224.
- 4 Demondion X, Bacqueville E, Paul C, Duquesnoy B, Hachulla E, Cotten A. Thoracic outlet: assessment with MR imaging in asymptomatic and symptomatic populations. *Radiology*. 2003 May;227(2):461–8.
- 5 Cejas C, Rollán C, Michelin G, Nogués M. High resolution neurography of the brachial plexus by 3Tesla magnetic resonance imaging. *Radiología (English Edition)*. 2016 Mar;58(2):88–100.

- 6 Singh VK, Jeyaseelan L, Kyriacou S, Ghosh S, Sinisi M, Fox M. Diagnostic value of magnetic resonance imaging in thoracic outlet syndrome. *J Orthop Surg (Hong Kong)*. 2014 Aug;22(2):228–31.
- 7 Demondion X, Herbinet P, Van Sint Jan S, Boutry N, Chantelot C, Cotten A. Imaging assessment of thoracic outlet syndrome. *Radiographics*. 2006 Nov;26(6):1735–50.
- 8 Demirbag D, Unlu E, Ozdemir F, Genchellac H, Temizoz O, Ozdemir H, et al. The Relationship Between Magnetic Resonance Imaging Findings and Postural Maneuver and Physical Examination Tests in Patients With Thoracic Outlet Syndrome: Results of a Double-Blind, Controlled Study. *Archives of Physical Medicine and Rehabilitation*. 88(7):844–51.
- 9 Cotten A, Demondion X, Gillard J, Hachulla E, Duquesnoy B. Exploration du défilé cervico-thoraco-brachial:apport de l'IRM. *La Revue de Médecine Interne*. 1999 Sep;20:478s–480s.
- 10 Poretti D, Lanza E, Sconfienza LM, Mauri G, Pedicini V, Balzarini L, et al. Simultaneous bilateral magnetic resonance angiography to evaluate thoracic outlet syndrome. *Radiol Med*. 2014 Oct 28.
- 11 Poretti D, Lanza E, Sconfienza LM, Mauri G, Pedicini V, Balzarini L, et al. Simultaneous bilateral magnetic resonance angiography to evaluate thoracic outlet syndrome. *Radiol Med*. 2014 Oct 28;120(5):407–12.
- 12 Ersoy H, Steigner ML, Coyner KB, Gerhard-Herman MD, Rybicki FJ, Bueno R, et al. Vascular Thoracic Outlet Syndrome: Protocol Design and Diagnostic Value of Contrast-

Enhanced 3D MR Angiography and Equilibrium Phase Imaging on 1.5- and 3-T MRI Scanners. *American Journal of Roentgenology*. 2012 May;198(5):1180–7.

13 Baumer P, Kele H, Kretschmer T, Koenig R, Pedro M, Bendszus M, et al. Thoracic outlet syndrome in 3T MR neurography-fibrous bands causing discernible lesions of the lower brachial plexus. *Eur Radiol*. 2014 Mar;24(3):756–61.

## FIGURE LEGENDS

**Figure 1:** Resection of the first rib and of a cervical rib

**Figure 2:** MRI, coronal T2 STIR view, Maximum Intensity Projection reformation in a 26-year-old female. Normal appearance of the brachial plexus with the root levels from C5 to T1 and the superior, middle, and inferior trunk levels (TS, TM, and TI, respectively). The T1 root and inferior trunk are in contact with the superior pleural sinus (AP).

**Figure 3:** Normal appearance of the brachial plexus. MRI, T1-weighted coronal view in a 32-year-old female.

(a) Interscalene triangle: emergence of the brachial plexus roots from C5 to T1. The C8 and T1 roots are in contact with the first rib (C1).

(b) Contents of the costoclavicular space: subclavian artery (A) and vein (V) and brachial plexus (N) between the first rib (C1) inferiorly and the clavicle (Clav) superiorly

**Figure 4:** Normal appearance of the brachial plexus. MRI, sagittal T1-weighted view of the thoracic outlet in a 32-year-old female

(a) Interscalene triangle: note the root levels from C5 to T1 between the anterior scalene muscle (SA) anteriorly and the middle and posterior scalene muscles (SM) posteriorly. Contact inferiorly with the subclavian artery (A).

(b) Costoclavicular space containing the subclavian artery (A) and vein (V) and the lateral, posterior, and medial bundles of the brachial plexus (FL, FP, and FM, respectively). Bordered superiorly by the clavicle (Clav), omohyoid muscle (OH), and subclavius muscle (SCI) and inferiorly by the first rib (C1)

(c) Retro-pectoralis minor space: the pectoralis minor muscle is in contact anteriorly with the artery (A), vein (V), and terminal branches of the brachial plexus (N)

**Figure 5:** Anatomical rib variant, MRI, coronal T1-weighted view of the costoclavicular space in a 45-year-old male. The brachial plexus (N) is displaced by a synchondrotic variant of the right first rib (C1)

**Figure 6:** Hypertrophy of the anterior scalene muscle, MRI, sagittal T1-weighted view of the scalene triangle in a 43-year-old male. Increased antero-posterior dimensions of the anterior scalene muscle (SA) with loss of peri-neural fat

**Figure 7:** Scalene muscle variant, MRI, coronal (a) and axial (b) T1-weighted views in a 39-year-old male. Supernumerary muscle head (\*) between the right anterior and middle scalene muscles in contact with the brachial plexus (N), with a distal attachment to the first rib (C1)

		Chirurgie	IRM
Compression retrouvée		48 (100%)	34(71%)
Site de compression	Mixte	44 (92%)	10 (21%)
	DIS isolé	4 (8%)	21 (44%)
	PCC isolée	0	3 (6%)
	TPP isolé	0	0
	Indéterminé	0	14 (29%)

**Tableau 1 : Nombre et différents sites de compressions extrinsèques de l'environnement osseux ou musculaires retrouvés en per opératoire et à l'IRM**



	Présence à l'IRM	Présence à la chirurgie	VP	FN	VN	FP	Sensibilité %	Spécificité %	VPP	VPN
<b>Bandes</b>	10	36	10	26	12	0	28 IC95[13-42]	100	100	32
<b>Cote cervicale</b>	3	3	3	0	45	0	100	100	100	100
<b>Apophyso mégalie</b>	0	0	0	0	48	0		100		100
<b>Anomalie clavicule/ cote</b>	0	2	0	2	45	0		100		96
<b>Hypertrophie SA</b>	25	26	21	5	18	4	81 IC95[65-95]	82 IC95[65-97]	84	78
<b>SA fibreux</b>	1	26	0	26	21	1		95 IC95[86-100]		45
<b>Hypertrophie SM</b>	13	33	13	20	15	0	39 IC95[22-56]	100	100	43
<b>SM fibreux</b>	0	11	0	11	37	0		100		77
<b>Muscle accessoire</b>	4	8	4	4	40	0	50 IC95[15-84]	100	100	90
<b>Hypertrophie SC</b>	7	3	3	0	41	4	100	91 IC95[82-91]	43	100
<b>Hypertrophie PP</b>	4	1	1	0	44	3	100	94 IC95[86-100]	25	100
<b>Ligament CC compressif</b>	0	6	0	6	42	0		100		87

**Tableau 2 : Sensibilité, spécificité, valeur prédictive positive et négative de l'IRM dans le diagnostic des éléments compressifs du STCTB**

SA : muscle scalène antérieur ; SM : muscle scalène moyen ; SC : muscle sous clavier ; PP : muscle petit pectoral ; CC : coraco-claviculaire ; VP : vrai positif ; FN : faux négatif ; VN : vrai négatif ; FP : faux positif ; IC95 : intervalle de confiance

	IRM 1,5 tesla (n=29)						IRM 3 tesla (n=19)					
	VP	FN	VN	FP	Sensibilité %	Spécificité %	VP	FN	VN	FP	Sensibilité %	Spécificité %
<b>Bandes</b>	8	16	5	0	33	100	2	10	7	0	16	100
<b>Hypertrophie SA</b>	12	4	10	3	75	77	9	1	8	1	90	89
<b>SA fibreux</b>	0	9	19	1		95	0	17	2	0		100
<b>Hypertrophie SM</b>	7	14	8	0	33	100	6	6	7	0	50	100
<b>Muscle accessoire</b>	2	2	25	0	50	100	2	2	15	0	50	100
<b>Hypertrophie SC</b>	2	0	24	3	100	89	1	0	17	1	100	94
<b>Hypertrophie pp</b>	0	0	26	3		90	1	0	18	0	100	100

**Tableau 3 : Caractéristiques des IRM 1,5 tesla et 3 tesla dans le diagnostic des éléments compressifs du STCTB.** SA : muscle scalène antérieur ; SM : muscle scalène moyen ; SC : muscle sous clavier ; PP : muscle petit pectoral ; VP : vrai positif ; FN : faux négatif ; VN : vrai négatif ; FP : faux positif



Figure 1



Figure 2

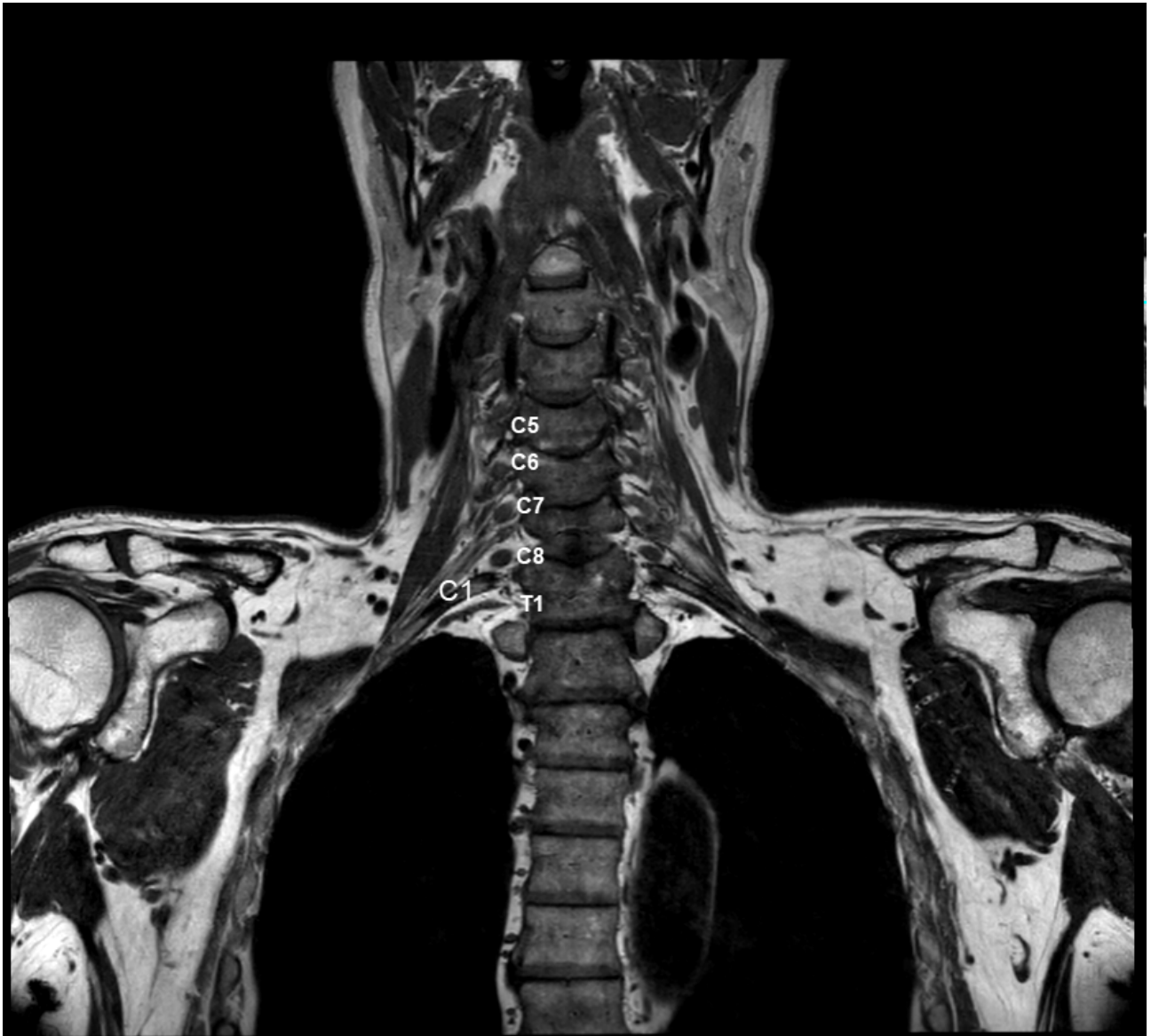


Figure 3a



Figure 3b

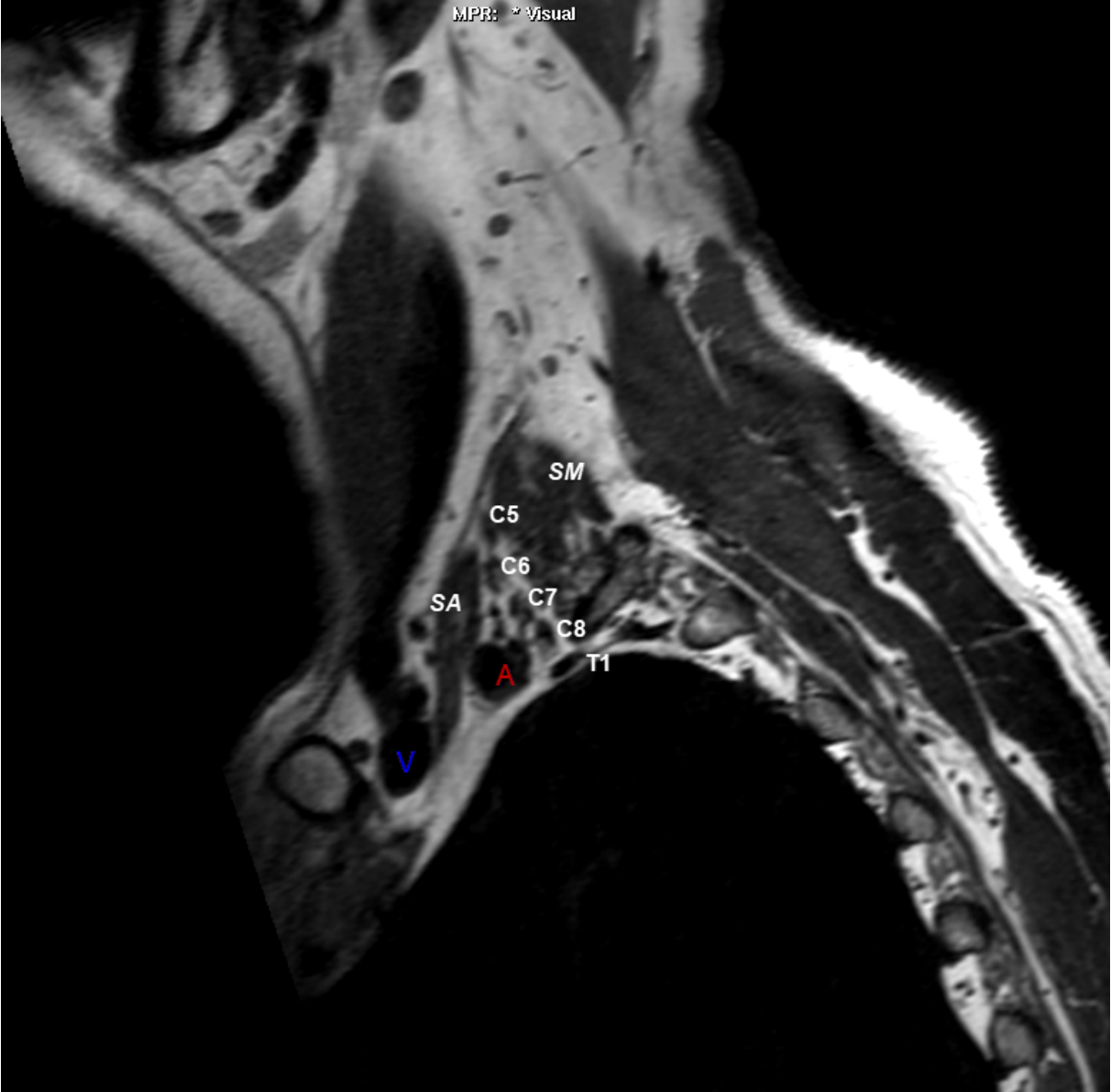


Figure 4a

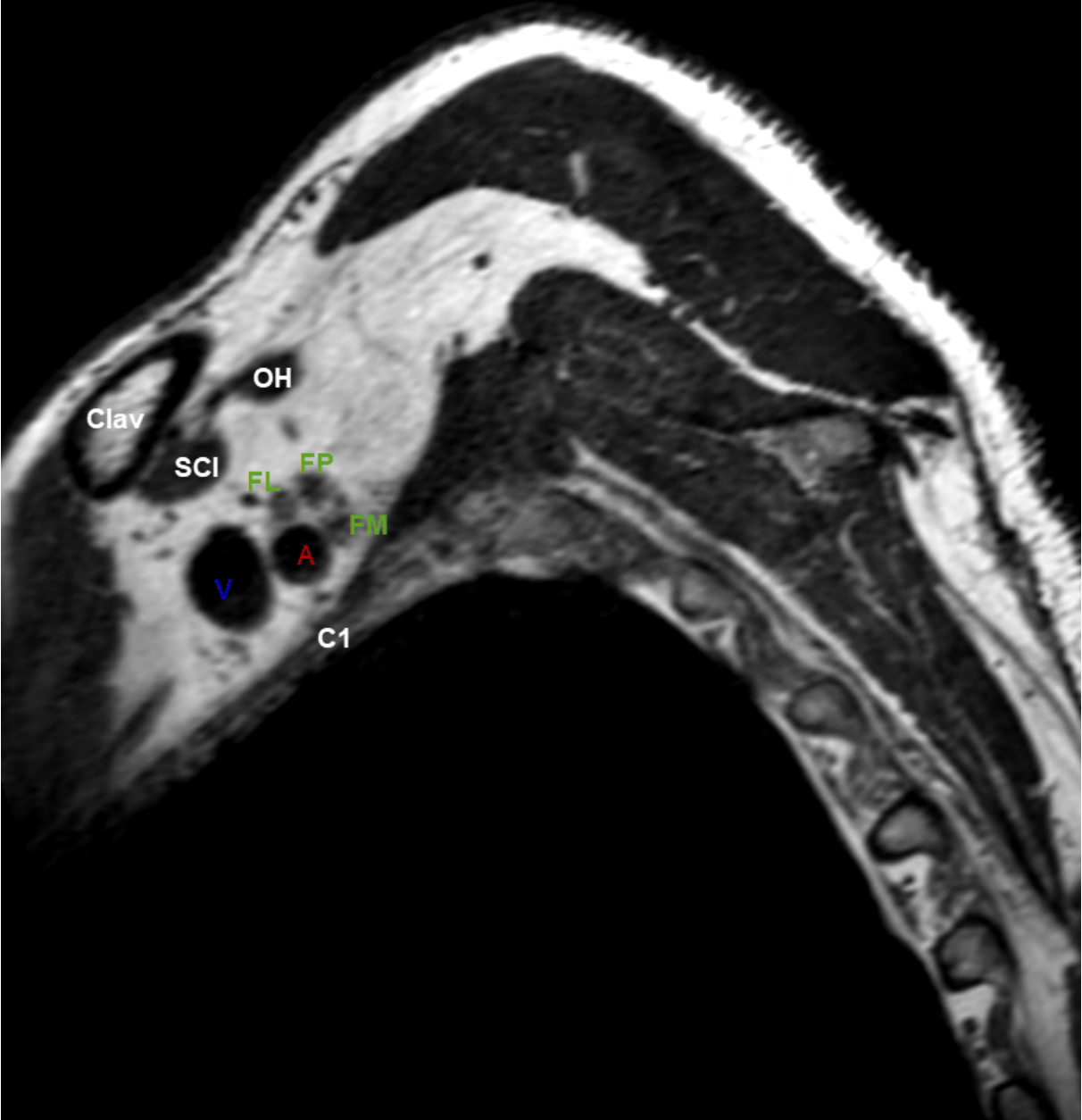


Figure 4b



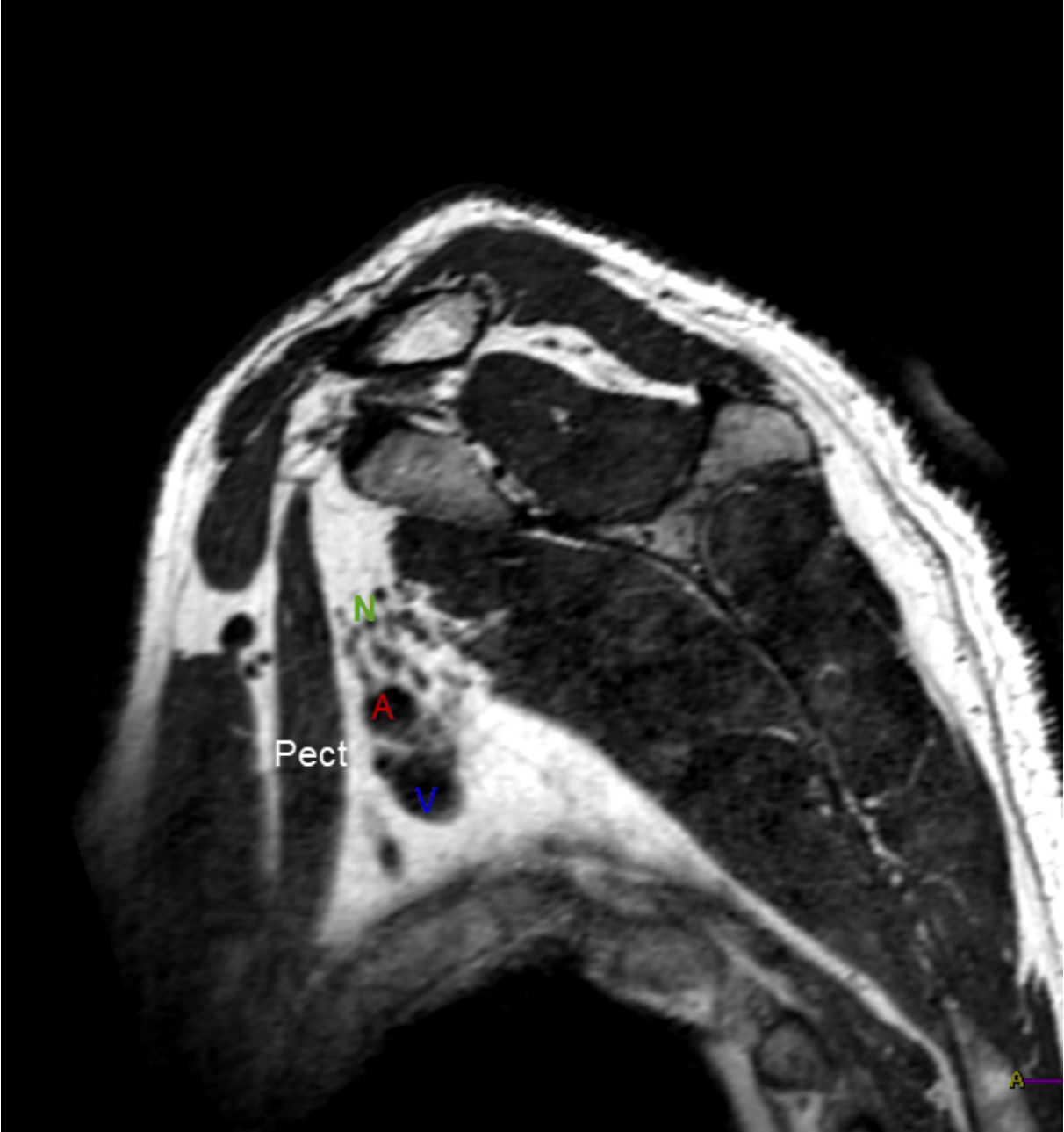


Figure 4c

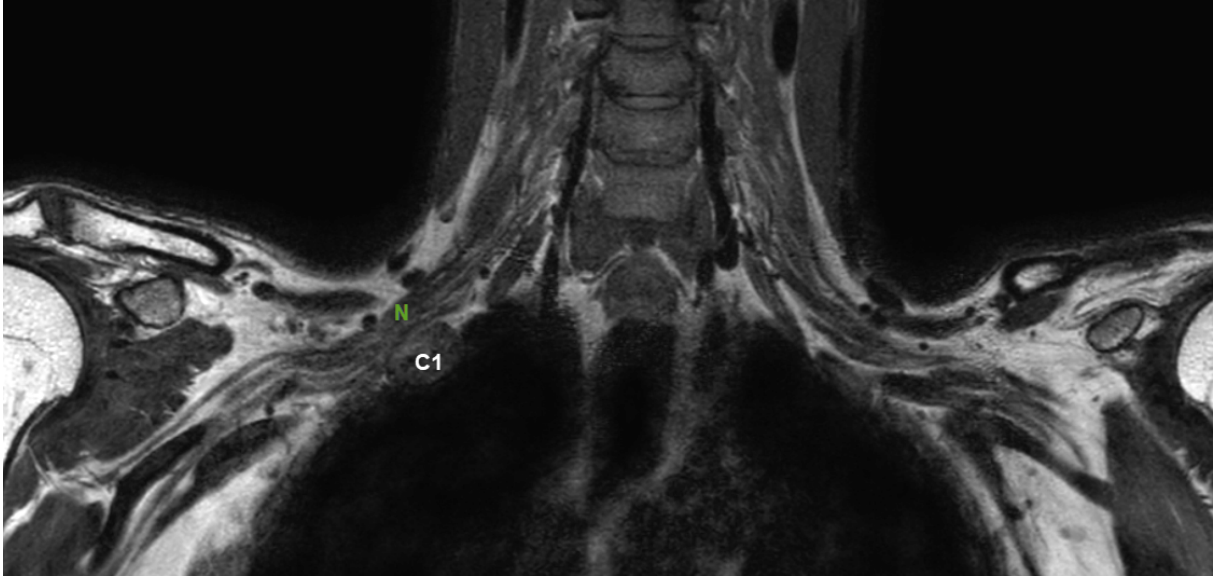


Figure 5

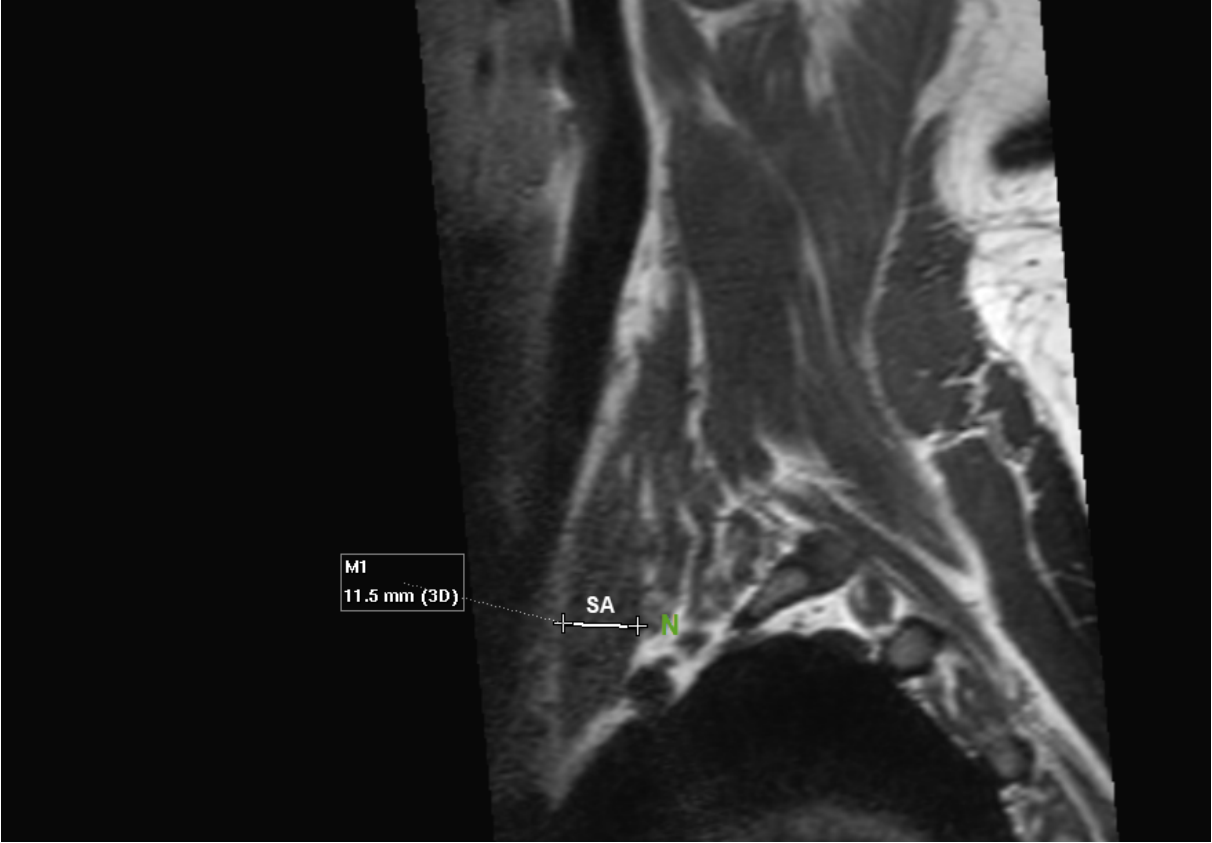


Figure 6

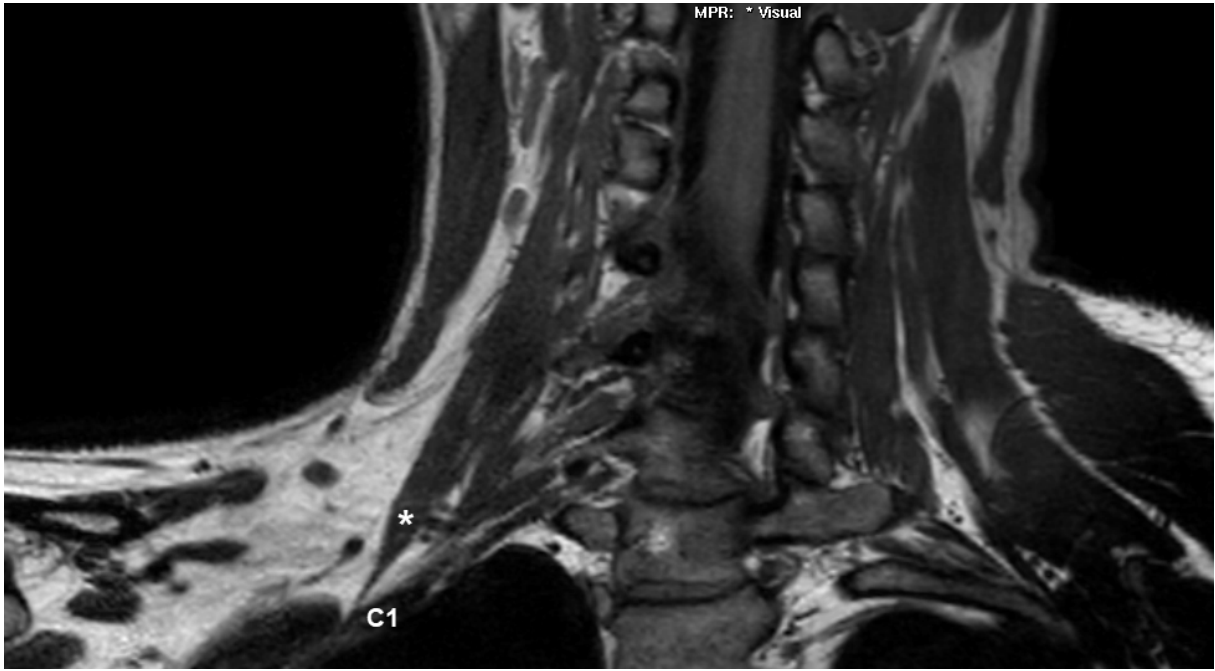


Figure 7a

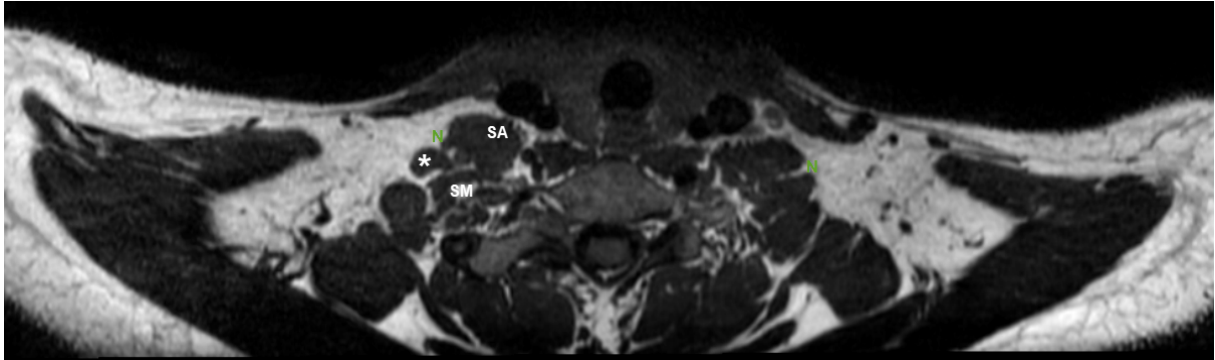


Figure 7b